photonics

MDPI

Article

Algebraic Absorption in Non-Hermitian Photonic Lattices

Stefano Longhi [1,2]

[1] Dipartimento di Fisica, Politecnico di Milano, Piazza L. da Vinci 32, I-20133 Milano, Italy; stefano.longhi@polimi.it
[2] Instituto de Física Interdisciplinar y Sistemas Complejos (IFIS-UIB), Campus Universitat de les Illes Balears, E-07122 Palma de Mallorca, Spain

Abstract

Non-Hermitian photonic lattices offer unconventional control over light evolution owing to modal non-orthogonality and the resulting non-normal dynamical response. In this work, we show that a uniform passive waveguide lattice with dissipation confined to one or a few sites near an edge can exhibit an algebraic(nearly linear) decay of optical power—an absorption law forbidden in orthogonal (normal-mode) dissipative systems, where any superposition of eigenmodes yields purely multi-exponential attenuation. We demonstrate that algebraic absorption arises when the input excitation is appropriately tailored to exploit non-orthogonal modal interference, effectively channeling energy toward the dissipative boundary. In particular, under the condition of coherent perfect absorption (CPA) associated with a spectral singularity of the semi-infinite lattice, nearly complete light absorption accompanied by algebraic decay of the optical power can be achieved. Starting from the minimal configuration of a single lossy edge site, we derive compact analytical expressions for the dynamics and identify the conditions under which linear-like absorption emerges. We then extend the analysis to multiple edge-proximal lossy sites. Our results show that simple dissipative photonic lattices, when driven by suitably prepared input states, enable robust sculpting of absorption laws through non-normal dynamics, providing a new route to programmable attenuation.

Keywords: non-Hermitian photonics; spectral singularities; absorption control

1. Introduction

Non-Hermitian photonic lattices have emerged as a powerful platform for controlling light propagation through engineered loss, gain, and modal non-orthogonality (see e.g., Refs. [1–10] and references therein). Such systems exhibit a wealth of behavior without Hermitian counterparts, including exceptional-point (EP) physics [1–6], spectral singularities [3,11–16], enhanced sensitivity [2,5,17], unidirectional transport [1–3], non-reciprocal mode conversion [2,18], transparency [19–21], perfect state transfer [22] and unconventional localization effects [23–30]. Among the many opportunities enabled by non-Hermiticity, shaping optical absorption is of central importance for applications in filtering, signal processing, and light–matter interactions. Traditional strategies rely on impedance matching and critical coupling in resonant structures [31–35], coherent perfect absorption (CPA) [36–51], quantum-engineered schemes [52,53], and temporal switching [54], which require precise spatial, spectral, or geometrical design of the absorber.

A distinctive feature of non-Hermitian lattices is the non-orthogonality of their eigenmodes, reflecting the non-normality of the underlying Hamiltonian [55–64]. Non-normal systems can exhibit transient growth [61,63], enhanced sensitivity to initial conditions

Check for updates

Received: 26 May 2026
Revised: 7 June 2026
Accepted: 10 June 2026
Published: 11 June 2026

Copyright: © 2026 by the author. Licensee MDPI, Basel, Switzerland. This article is an open access article distributed under the terms and conditions of the Creative Commons Attribution (CC BY) license.

and excess noise [55,56,59–62], and anomalous relaxation dynamics [65,66]. These effects originate from interference among non-orthogonal modes and can strongly modify the evolution of energy and coherence in extended photonic structures. Yet the question of how absorption itself can be engineered in extended non-normal systems—particularly when loss is sparse or confined to a small region—remains largely open. In particular, the possibility of realizing absorption laws that fundamentally depart from both standard Lambert–Beer attenuation and generic multi-exponential decay has received little attention. Such unconventional absorption laws are of interest because they enable a controlled redistribution of energy dissipation along the propagation direction. In contrast to exponential attenuation, which rapidly depletes the optical power at short propagation distances and leaves a long residual tail, algebraic decay can provide a more uniform absorption rate, potentially offering new opportunities for power management, signal conditioning, and wave-control applications in integrated photonic platforms.

In this work, we show that algebraic (nearly linear) optical power decay can arise in a remarkably simple setting: a uniform passive lattice with dissipation localized at one or a few sites near an edge. Such an absorption law is forbidden in normal-mode systems, where orthogonal eigenmodes enforce purely multi-exponential decay for any initial condition. Here we demonstrate that breaking modal orthogonality in non-normal non-Hermitian lattices allows suitably tailored input excitations to redistribute energy into channels that are efficiently funneled toward the dissipative boundary. This enables a coherent perfect absorption (CPA)-like mechanism emerging at a spectral singularity of the semi-infinite lattice. In this regime, excitation directed toward the lossy edge is fully absorbed through constructive interference of non-orthogonal scattering states, giving rise to robust algebraic attenuation over long propagation distances. When the CPA condition is not satisfied, algebraic decay persists only up to a finite propagation length, beyond which the absorption rate is strongly reduced.

Starting from the minimal configuration of a single lossy edge site, we derive compact analytical expressions for the dynamics and identify the conditions under which linear-like absorption emerges. We then extend the analysis to multiple lossy sites near the boundary and uncover a systematic trend: increasingly robust algebraic decay and nearly complete absorption are obtained as the system approaches a spectral singularity in the semi-infinite limit, corresponding to a CPA-like condition. These results establish that minimal dissipative photonic lattices, combined with tailored input excitation, provide a fundamentally new route to control optical absorption. They enable programmable attenuation laws beyond exponential decay and identify non-normality and spectral singularities as key physical resources for wave control in non-Hermitian photonic systems.

2. Absorption Law in Dissipative Waveguide Lattices: General Formulation

We consider a dissipative waveguide lattice comprising L waveguides with the uniform coupling constant J between adjacent waveguides and site-dependent loss rates γ_n. Typically, only a few lossy sites are present near the left edge $n = 1$ of the lattice, as schematically shown in Figure 1a. Light propagation is governed by the coupled-mode equations for the modal field amplitudes $\psi_n(z)$ along the propagation coordinate z,

$$i\frac{d\psi_n}{dz} = J(\psi_{n+1} + \psi_{n-1}) - i\gamma_n\psi_n, \tag{1}$$

with the open boundary conditions $\psi_0 = \psi_{L+1} = 0$. Introducing the state vector $|\psi(z)\rangle = (\psi_1(z), \psi_2(z), \ldots, \psi_L(z))^T$, the dynamics can be written as

$$i\frac{d}{dz}|\psi(z)\rangle = H\,|\psi(z)\rangle, \tag{2}$$

where H is a finite-dimensional non-Hermitian Hamiltonian. We assume that H is diagonalizable, i.e., there are not EPs. The right and left eigenvectors are defined by

$$H|R^{(\alpha)}\rangle = \lambda_\alpha|R^{(\alpha)}\rangle, \qquad H^\dagger|L^{(\alpha)}\rangle = \lambda_\alpha^*|L^{(\alpha)}\rangle, \tag{3}$$

and satisfy the biorthogonality relation

$$\langle L^{(\beta)}|R^{(\alpha)}\rangle = \delta_{\alpha\beta}. \tag{4}$$

We further assume that all modes are decaying, i.e., $\mathrm{Im}(\lambda_\alpha) < 0$. This means that the lattice does not support "dark states", i.e., all right eigenmodes display non-vanishing amplitude at some of the lossy sites. A sufficient condition to avoid dark states is to have some loss at the boundary site $n = 1$. The field can be expanded as a superposition of super-modes as

$$|\psi(z)\rangle = \sum_{\alpha=1}^{L} c_\alpha\, \exp(-i\lambda_\alpha z)|R^{(\alpha)}\rangle \tag{5}$$

with spectral amplitudes $c_\alpha = \langle L^{(\alpha)}|\psi(0)\rangle$. The total optical power at propagation distance z is given by

$$P(z) = \langle\psi(z)|\psi(z)\rangle = \sum_{n=1}^{L}|\psi_n(z)|^2, \tag{6}$$

which evaluates to

$$P(z) = \sum_{\alpha,\beta} c_\alpha c_\beta^*\, \exp[-i(\lambda_\alpha - \lambda_\beta^*)z]\langle R^{(\beta)}|R^{(\alpha)}\rangle. \tag{7}$$

This expression shows that the dynamics is generally governed by interference between non-orthogonal super-modes. The overlap matrix $\langle R^{(\beta)}|R^{(\alpha)}\rangle$ couples different modal contributions, so that the power evolution is not, in general, a simple sum of independent decaying exponentials.

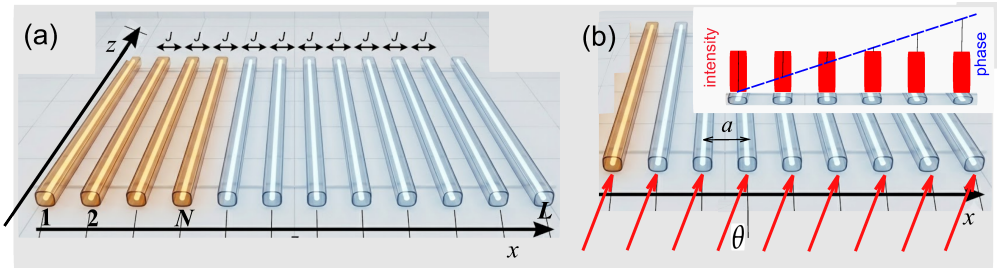


Figure 1. (**a**) Schematic of an array of uniformly spaced, evanescently coupled optical waveguides. The array comprises L waveguides, with a small number of lossy waveguides located near the left edge. The coupling constant between adjacent waveguides is J, and the loss rate of the n-th waveguide is γ_n, where $\gamma_n = 0$ for $n > N$ and $N \ll L$. (**b**) Excitation geometry corresponding to the CPA condition at the Bloch wave number $q = \pi/2$. The array is illuminated by a plane wave incident at the Bragg angle $\theta = \lambda/(2a)$, where a is the lattice period (waveguide spacing) and λ is the optical wavelength.As shown in the inset, this excitation corresponds to a uniform intensity profile combined with a linear phase gradient, featuring a $\pi/2$ phase shift between adjacent waveguides.

In the special case where H is normal, i.e., when $HH^\dagger = H^\dagger H$, the right eigenvectors form an orthonormal basis and coincide (up to phase) with the left eigenvectors,

$$\langle R^{(\beta)}|R^{(\alpha)}\rangle = \delta_{\alpha\beta}, \qquad |L^{(\alpha)}\rangle = |R^{(\alpha)}\rangle. \tag{8}$$

In this case all interference terms vanish and the power reduces to a purely multi-exponential form,

$$P(z) = \sum_{\alpha=1}^{L} |c_\alpha|^2 \exp[2\,\mathrm{Im}(\lambda_\alpha)\, z]. \tag{9}$$

Thus, in normal (orthogonal-mode) systems, the absorption dynamics is always a weighted sum of exponential decays determined solely by the eigenvalue spectrum, and no algebraic power laws, such as linear attenuation, can emerge. In fact, one has

$$\frac{dP}{dz} = 2\sum_{\alpha=1}^{L} |c_\alpha|^2\, \mathrm{Im}(\lambda_\alpha)\, \exp[2\,\mathrm{Im}(\lambda_\alpha)\, z], \tag{10}$$

which is a sum of strictly decaying exponential contributions with negative coefficients. Consequently, dP/dz cannot remain constant or approximately approach a z-independent value, and therefore the total power decay cannot follow an algebraic law over extended propagation distances. In addition, in a normal system there are strict upper and lower bounds for the decay law $P(z)$. Define the decay rates as $\kappa_\alpha = -\mathrm{Im}(\lambda_\alpha) > 0$. Since each term decays independently, the total power is bounded by the extremal decay rates of the spectrum. Defining $\kappa_{\min} = \min_\alpha \kappa_\alpha, \kappa_{\max} = \max_\alpha \kappa_\alpha$, one obtains the bounds

$$P(0)\exp(-2\kappa_{\max} z) \;\le\; P(z) \;\le\; P(0)\exp(-2\kappa_{\min} z). \tag{11}$$

In contrast, in non-normal systems the interference terms between non-orthogonal modes fundamentally modify this structure, enabling qualitatively new decay behaviors, including the algebraic absorption laws discussed in this work, as well as breakdown of the bounds in Equation (11). Departure from non-normality of the Hamiltonian H can be characterized by several indicators, including Petermann factor, condition number of eigenvectors, pseudospectrum, Kreiss constant and Henrici's departure from normality (see e.g., ref [67]). For networks, a useful parameter is provided by the Henrici number [67,68]

$$\nu = \left(\|H\|_F^2 - \sum_{\alpha=1}^{N} |\lambda_\alpha|^2 \right)^{1/2}$$

and its normalized value $\nu_N = \nu/\|H\|_F$, where $\|H\|_F \equiv \sqrt{\sum_{n,m=1}^{N} |H_{n,m}|^2}$ is the Frobenius norm of H. The normalized Henrici parameter ν_N is scale invariant and satisfies the condition $0 \le \nu_N \le 1$, with $\nu_N = 0$ if and only if the matrix H is normal. Hence ν_N provides a global measure of non-normality, with $\nu_N = 1$ for extreme non-normality, when all eigenvalues of H are zero (e.g., a nilpotent Jordan block).

We finally note that, for the specific dissipative Hamiltonian considered here, the power evolution $P(z)$ can be equivalently written as

$$\frac{dP(z)}{dz} = -2\sum_n \gamma_n\, |\psi_n(z)|^2 \quad \rightarrow \quad P(z) = P(0) - 2\sum_n \gamma_n \int_0^z dz' |\psi_n(z')|^2. \tag{12}$$

This expression shows that the total absorption is entirely determined by the local intensity at the lossy sites, so that the global decay law is governed solely by the evolution of the modal amplitudes on those sites.

3. Algebraic Absorption from a Single Lossy Boundary Site

We first analyze the minimal realization of the proposed mechanism: a waveguide lattice with dissipation localized at a single boundary site ($\gamma_n = \gamma$ for $n = 1$ and $\gamma_n = 0$ otherwise). Despite its simplicity, this configuration already captures the essential physics underlying non-normal absorption and its connection to coherent perfect absorption (CPA) and spectral singularities. According to Equation (12), the optical power $P(z)$ satisfies

$$\frac{dP}{dz} = -2\gamma|\psi_1(z)|^2, \tag{13}$$

showing that the global decay is fully determined by the intensity at the lossy edge site. In this way, engineering the evolution of $|\psi_1(z)|^2$ allows, in principle, one to design a target absorption law $P(z)$ through a suitable choice of the initial excitation $\psi_n(0)$. To construct such solutions, we first consider the semi-infinite limit $L \to \infty$ and prescribe a desired evolution for $\psi_1(z)$ consistent with a target power decay law $P(z)$. The coupled-mode Equations (1) can then be rewritten in recursive form as

$$\psi_2(z) = \frac{i}{J}\frac{d\psi_1}{dz} + i\frac{\gamma}{J}\psi_1(z), \tag{14}$$

$$\psi_{n+1}(z) = \frac{i}{J}\frac{d\psi_n}{dz} - \psi_{n-1}(z), \qquad (n \geq 2). \tag{15}$$

These relations allow one to recursively determine $\psi_n(z)$ for all $n = 2, 3, 4, \ldots$, and in particular to reconstruct the input field distribution $\psi_n(0)$ at the excitation plane $z = 0$. In general, the resulting sequence $\psi_n(0)$ is non-vanishing and may even exhibit secular growth with increasing n or singularities. In a finite lattice, physical realizability requires truncation at site L, with the boundary condition $\psi_{L+1} = 0$. Admissible solutions are therefore those for which $\psi_n(0)$ remains bounded as n increases.

Importantly, in the truncated system the prescribed evolution of $\psi_1(z)$—and hence the designed power law $P(z)$—is accurately realized only up to a finite propagation distance. Beyond this scale, reflections from the opposite boundary at $n = L$ spoil the intended dynamics. To estimate the corresponding crossover distance z^*, we note that excitations propagate through the lattice with a maximal group velocity bounded by the Lieb–Robinson velocity $v_g = 2J$. Consequently, the influence of the boundary at $n = L$ reaches the lossy edge site $n = 1$ only after a propagation distance

$$z^* \simeq \frac{L}{2J}. \tag{16}$$

For $z < z^*$, the evolution of $\psi_1(z)$ is essentially unaffected by finite-size effects, and the engineered absorption law $P(z)$ is faithfully reproduced over this interval.
We now specialize the absorption-sculpting protocol to the case of a linear decay law

$$P(z) = P(0) - 2\alpha z, \tag{17}$$

where $2\alpha > 0$ is the slope of the linear attenuation. According to Equation (13), this behavior is obtained by choosing

$$\psi_1(z) = \sqrt{\frac{\alpha}{\gamma}}, \tag{18}$$

i.e., a z-independent boundary amplitude. The recursion relations (14)–(15) can then be solved explicitly, yielding the following initial excitation condition:

$$|\psi(0)\rangle = \sqrt{\frac{\alpha}{\gamma}}\left(1, i\frac{\gamma}{J}, -1, -i\frac{\gamma}{J}, 1, i\frac{\gamma}{J}, \dots\right). \tag{19}$$

For a truncated lattice of size $L \gg 1$, the initial optical power is approximately

$$P(0) \simeq \frac{\alpha L}{\gamma}\frac{1+(\gamma/J)^2}{2}, \tag{20}$$

and the linear decay (17) is realized up to the propagation distance $z^* \simeq L/(2J)$. At $z = z^*$, the residual optical power reads

$$P(z^*) = P(0) - 2\alpha z^* \simeq \frac{\alpha L}{2\gamma}\left(\frac{\gamma}{J} - 1\right)^2, \tag{21}$$

which is manifestly non-negative and vanishes when $J = \gamma$. In this case, all the optical power is absorbed at the edge lossy site $n = 1$, and a coherent perfect absorption (CPA) condition is realized. Remarkably, under the CPA condition $\gamma = J$, the initial waveguide array excitation that realizes the algebraic power decay is very simple: uniform (plane wave) intensity illumination tilted at the Bragg angle $\theta = \lambda/(2a)$, corresponding to $q = \pi/2$, where λ is the wavelength of injected light and a the lattice period (distance between adjacent waveguides); see Figure 1b for a schematic.

For $z > z^*$, the decay law $P(z)$ departs from the linear behavior because of finite-size reflections originating from the distant lattice boundary. When the CPA condition at $q = \pi/2$ is not fulfilled, the residual optical power remaining in the lattice for $z > z^*$ decays only slowly, at a rate determined by the smallest decay exponent $\kappa_{\min}$. Figure 2 shows numerical results obtained by integrating the coupled-mode equations, Equation (1), with the initial condition (19) for both $\gamma \neq J$ [Figure 2a,b] and $\gamma = J$ [Figure 2c]. The thin burgundy dashed curves correspond to the predicted linear decay law (17), which accurately reproduces the exact dynamics in the finite lattice up to the propagation length z^* given by Equation (16). Remarkably, the linear-decay regime exhibits a behavior that can violate the bound (11) characteristic of normal Hamiltonians [Figure 2a,c], and for $\gamma = J$ the numerical results confirm the near-complete absorption predicted by theory. Conversely, for $\gamma \neq J$ the residual optical power decays at a much slower rate for $z > z^*$, as illustrated in Figure 2a,b.

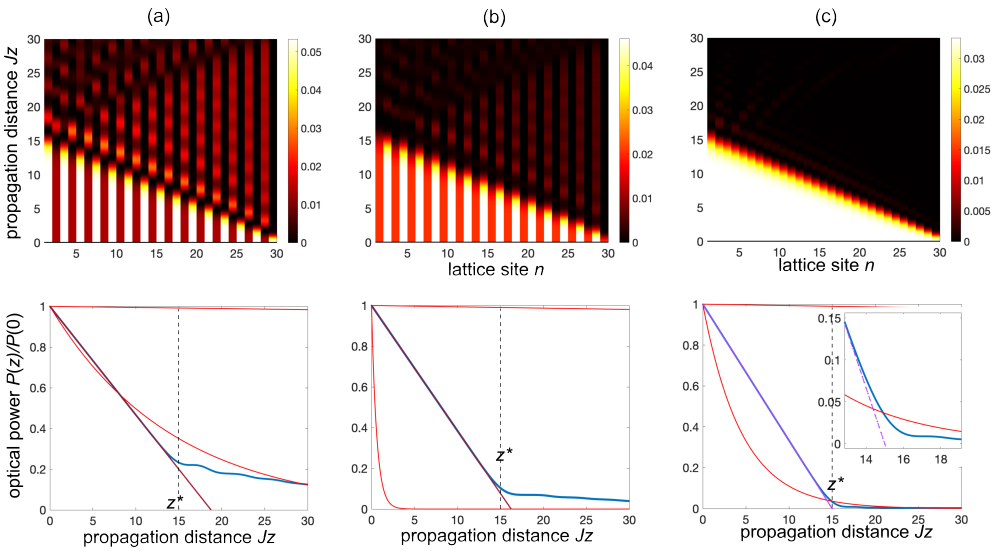


Figure 2. Light dynamics in a waveguide array comprising $L = 30$ waveguides with one boundary lossy waveguide for a few increasing values of the ratio γ/J. (**a**) $\gamma/J = 0.5$, (**b**) $\gamma/J = 1.5$, and

(**c**) $\gamma/J = 1$, corresponding to CPA at the Bloch wave number $q = \pi/2$. The normalized Henrici parameter in the three cases, from (**a**) to (**c**), is $\nu_N = 0.0091$, $\nu = 0.0272$ and $\nu = 0.0181$, respectively. Upper panels show the light intensity propagation along the z axis on a pseudocolor map, whereas the lower panels (blue bold curves) show the numerically-computed decay dynamics of the total optical power $P(z)$. Initial array excitation is given by Equation (19). The thin red curves show the exponential decay curves corresponding to the most and less damped super-modes, whereas the thin burgundy dashed curve shows the linear (algebraic) decay predicted by the theoretical analysis. The propagation distance z^*, above which the power decay deviates from the linear theoretical prediction, is indicated by the vertical dashed curves and reads $z^* = L/(2J)$. The inset in (**c**) is an enlargement of the decay curves near $z = z^*$.

4. Algebraic Absorption from Multiple Lossy Boundary Sites: CPA and Spectral Singularities

We now extend the analysis to the case where dissipation is distributed over a small number of sites near the lattice boundary $n \simeq 1$, rather than being confined to a single edge waveguide. This generalization preserves the essential physical mechanism identified in the previous section, namely the interplay between non-orthogonal super-modes and boundary-directed energy flow, while enriching the physics underlying the emergence of linear absorption laws. In this broader setting, the appearance of algebraic absorption can be naturally interpreted in terms of the scattering process at the lossy edge region of a semi-infinite lattice and the associated formation of a coherent perfect absorption (CPA) condition. Such CPA states correspond to specific input excitations that are fully absorbed by the lossy boundary region, with vanishing outgoing flux. In the present framework, they arise at or in the vicinity of spectral singularities of the associated semi-infinite non-Hermitian lattice.

Let us consider the model defined by Equation (1) and assume that $\gamma_n = 0$ for $n > N$, with $\gamma_N > 0$ and $N \ll L$. This means that the lossy sites are concentrated near the left edge $n = 1$ of the waveguide array. In the semi-infinite lattice limit $L \to \infty$, let us search for undamped scattering solution to the coupled-mode Equations (1) of the form $\psi_n(z) = u_n \exp(-iEz)$, with

$$Eu_n = J(u_{n+1} + u_{n-1}) - i\gamma_n u_n \tag{22}$$

and with the asymptotic behavior

$$u_n = \sqrt{P_0}\{\exp[iq(n-N)] + r(q)\exp[-iq(n-N)]\} \tag{23}$$

for $n \geq N$. In the above equations, $0 < q < \pi$ is the Bloch wave number of the incident wave propagating toward the lattice edge $n = 1$ with the group velocity $v_g = 2J\sin q$, $r(q)$ is the reflection coefficient, $E = 2J\cos q$ is the propagation constant and $\sqrt{P_0}$ the amplitude of the incident wave. The value of $r(q)$, as well as of the amplitudes u_n for $1 \leq n < N$, can be determined by standard transfer matrix methods (see e.g., Refs. [21,69]). After writing Equation (22) in the matrix form

$$\begin{pmatrix} u_{n+1} \\ u_n \end{pmatrix} = \begin{pmatrix} \frac{E+i\gamma_n}{J} & -1 \\ 1 & 0 \end{pmatrix} \begin{pmatrix} u_n \\ u_{n-1} \end{pmatrix} \equiv T_n \begin{pmatrix} u_n \\ u_{n-1} \end{pmatrix} \tag{24}$$

with $u_0 = 0$, one has

$$\begin{pmatrix} u_{N+1} \\ u_N \end{pmatrix} = Q \begin{pmatrix} u_1 \\ 0 \end{pmatrix} \tag{25}$$

where we have set $Q = T_N \times T_{N-1} \times ... \times T_1$. Substitution of the ansatz (23) into Equation (25) yields a linear system of equations for $r(q)$ and u_1, which is solved as

$$r(q) = \frac{Q_{11} - Q_{21}\exp(iq)}{Q_{21}\exp(-iq) - Q_{11}}, \quad u_1 = -\frac{2i\sin q}{Q_{21}\exp(-iq) - Q_{11}}\sqrt{P_0} \tag{26}$$

where $Q_{11}(q), Q_{12}(q), Q_{21}(q), Q_{22}(q)$ are the elements of the matrix $Q = Q(q)$. This analysis is exact one and the fact that the scattering solution is not damped in spite of the lossy sites is due to the fact that the solution carriers an infinite power (it is not normalizable). The continuous flow of optical power carried by the incident wave, propagating at the speed v_g is reflected by the fraction $|r|^2$ by the lattice boundary, while the fraction $(1 - |r|^2)$ is absorbed by the lossy sites. Hence, the rate 2α of absorbed power in the lossy sites, i.e., per unit of propagation distance along the axis z, is given by

$$2\alpha = P_0(1 - |r|^2)v_g. \tag{27}$$

The semi-infinite lattice exhibits CPA whenever $r(q) = 0$ at some incident Bloch wave number q. Such a vanishing of reflection corresponds to a spectral singularity of the non-Hermitian Hamiltonian of the semi-infinite lattice [13].

Let us now truncate the lattice at the right side assuming $u_n = 0$ for $n > L$, with $L \gg N$. In this case the optical power $P(z)$ carried by the optical beam is finite and at the input plane z it reads $P(0) = \sum_{n=1}^{L} |u_n|^2 \simeq P_0(1 + |r|^2)L$. Since the power $P(z)$ depends solely on the amplitudes $\psi_n(z)$ in the lossy sites (i.e., for $n < N$), and since such amplitudes $\psi_n(z)$ in the truncated lattice are well approximated by the ones of the infinite lattice up to the propagation distance $z^* \simeq L/(2J)$, for $z < z^*$ the rate of absorbed power can be estimated as $(dP/dz) \simeq -2\alpha = -(1 - |r|^2)P_0 v_g$, where we used Equation (27). This yields the linear (algebraic) decay law of the optical power $P(z) = P(0) - 2\alpha z$, i.e.,

$$P(z) \simeq P(0) - (1 - |r|^2)P_0 v_g z = P(0)\left(1 - \frac{v_g z}{L}\frac{1 - |r|^2}{1 + |r|^2}\right) \tag{28}$$

where $v_g = 2J\sin q$ is the transverse group velocity of the incoming wave. Equation (28) is valid up to the propagation distance $z^* \simeq L/(2J)$. The residual optical power at plane $z = z^*$ then reads

$$P(z^*) \simeq P(0)\left(1 - \sin q\frac{1 - |r|^2}{1 + |r|^2}\right). \tag{29}$$

Equation (29) clearly indicates that the injected optical power is fully absorbed after the propagation distance $z = z^*$ provided that $r(q) = 0$ and $q = \pi/2$, corresponding to a CPA effect in the semi-infinite lattice: all incoming optical radiation is not reflected by the lattice edge and fully absorbed by the lossy sites. We remark that the CPA condition $r(q) = 0$ of the semi-infinite lattice is a necessary, but not sufficient, condition to get fully absorbed optical power at $z = z^*$ in the truncated lattice: the additional requirement $\sin q = 1$, i.e., $q = \pi/2$, is required. This point will be illustrated in some numerical results discussed below. The special and minimal setting discuss in Section 2 can be obtained as a special case of the general analysis by assuming $\gamma_1 = \gamma$ and $\gamma_n = 0$ for $n \geq 1$. In this case the spectral reflection coefficient $r(q)$ in the scattering problem on the semi-infinite lattice can be readily calculated and reads

$$r(q) = -\frac{J\exp(-iq) + i\gamma}{J\exp(iq) + i\gamma}. \tag{30}$$

From this equation, it follows that the CPA condition $|r(q)| = 0$ occurs at $q = \pi/2$ whenever $\gamma = J$, in agreement with the results of Section 2. It is worth emphasizing that the algebraic

decay reported here is not an asymptotic property of a finite lattice. Rather, it emerges over a broad propagation interval whose extent is determined by the system size and by the proximity to the CPA condition. In finite arrays, the decay eventually crosses over to a slower relaxation regime once the wave packet has interacted with the lattice boundaries. However, the propagation distance over which the algebraic behavior is observed increases with the lattice size and becomes unbounded in the semi-infinite limit. Therefore, the effect should be regarded as a robust mesoscopic manifestation of non-normal dynamics rather than a finite-size artifact.

As an illustrative application of the general formalism, which extends the minimal model discussed in Section 2, we consider the case of N contiguous lossy sites at the edge of the waveguide lattice, all characterized by the same loss rate, i.e., $\gamma_n = \gamma$ for $n \leq N$ and $\gamma_n = 0$ for $n > N$. We aim to determine whether, and for which value of γ, the CPA condition can be satisfied at $q = \pi/2$. For $q = \pi/2$, corresponding to $E = 0$, the transfer matrix of the scattering region reads

$$Q = \begin{pmatrix} \frac{i\gamma}{J} & -1 \\ 1 & 0 \end{pmatrix}^N. \tag{31}$$

Since Q is unimodular, its N-th power can be evaluated analytically using the Cayley–Hamilton–Sylvester formula. In particular, the relevant matrix elements take the form

$$Q_{11} = i\frac{\gamma}{J}\sin(N\theta) - \sin[(N-1)\theta], \qquad Q_{21} = \sin(N\theta), \tag{32}$$

where the complex angle θ is defined by

$$\cos\theta = \frac{i\gamma}{2J}. \tag{33}$$

The CPA condition at $q = \pi/2$ requires vanishing reflection, which here reduces to

$$Q_{11} = i\,Q_{21}. \tag{34}$$

Introducing the parametrization $\theta = -\pi/2 + i\psi$ and using Equation (32), the CPA condition (34) reduces to the transcendental equations

$$\cosh\big[(N+1)\psi\big] = \sinh(N\psi), \qquad N \text{ even}, \tag{35}$$

and

$$\sinh\big[(N+1)\psi\big] = \cosh(N\psi), \qquad N \text{ odd}. \tag{36}$$

Equation (35) has no real solution for ψ, implying that CPA at $q = \pi/2$ cannot be achieved for even N. In contrast, for odd N, Equation (36) admits a unique solution $\psi > 0$, which can be determined numerically. In this case, the CPA condition $|r(q)| = 0$ at $q = \pi/2$ is satisfied provided that the loss rate is tuned to

$$\gamma = 2J\sinh\psi \equiv \gamma^*. \tag{37}$$

As an illustrative example, Figure 3 shows the numerically computed reflection coefficient $r(q)$ for $N = 3$ and increasing values of the loss rate, clearly indicating the emergence of CPA at $q = \pi/2$ when $\gamma = \gamma^*$, corresponding to $\psi \simeq 0.281$ and $\gamma^* \simeq 0.569J$. Figure 4 reports numerical simulations of the power evolution $P(z)$ for a lattice of $L = 30$ waveguides, with initial conditions chosen according to Equations (23) and (24). At $\gamma = \gamma^*$, the power decays almost linearly with z, and complete absorption is achieved at $z = z^* = L/(2J)$.

For $\gamma \neq \gamma^*$, residual reflection occurs; nevertheless, the linear decay persists up to $z = z^*$, beyond which the dynamics crosses over to a slower decay regime for $z > z^*$.

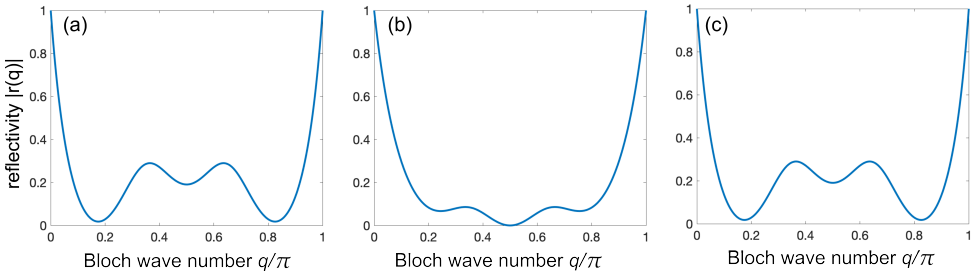


Figure 3. Numerically-computed spectral reflection $|r(q)|$ in a semi-infinite lattice with $N = 3$ lossy sites ($\gamma_1 = \gamma_2 = \gamma_3 = \gamma$, $\gamma_n = 0$ for $n > 3$) for a few increasing values of the ratio γ/J. (**a**) $\gamma/J = 0.2$, (**b**) $\gamma/J = \gamma^*/J = 2\sinh(0.281) \simeq 0.5694$, and (**c**) $\gamma/J = 1$. The case (**c**) corresponds to the CPA condition at $q = \pi/2$.

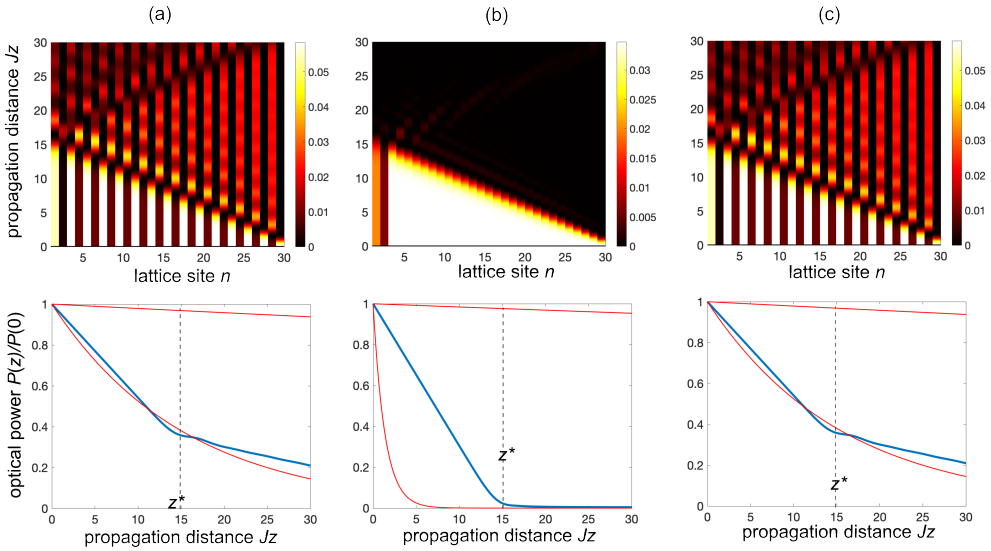


Figure 4. Same as Figure 2, but in a lattice with $N = 3$ lossy sites ($\gamma_1 = \gamma_2 = \gamma_3 = \gamma$ and $\gamma_n = 0$ for $n > N = 3$). The loss rate is $\gamma/J = 0.2$ in (**a**), $\gamma/J = \gamma^*/J \simeq 0.5694$ in (**b**), and $\gamma/J = 1$ in (**c**). The normalized Henrici parameter in the three cases, from (**a**) to (**c**), is $\nu_N = 0.0061$, $\nu_N = 0.0172$ and $\nu_N = 0.0303$, respectively.

For N even, although the CPA condition cannot be satisfied at $q = \pi/2$, it can be achieved for $q = q^* \neq \pi/2$, as illustrated in Figure 5a. In this case, excitation of the finite lattice by a single Bloch wave with wave number $q = q^*$ does not generate any reflected wave. However, at $z = z^*$ a residual amount of optical power remains trapped in the array, and further propagation is required for its complete absorption, which proceeds with a slower, non-algebraic decay, as shown in Figure 5b.

As a final comment, it should be noticed that the normalized Henrici parameter ν_N for the simulations shown in Figures 2, 3 and 5 varies in the interval $(0.001, 0.03)$. Such relatively modest values of ν_N highlight an important point: the algebraic-decay phenomenon is rooted to CPA and does not require an extremely large degree of non-normality, nor operation in the vicinity of exceptional points. This shows that the algebraic absorption mechanism is a rather robust consequence of CPA in the semi-infinite lattice limit and does not rely on fine tuning toward highly singular spectral degeneracies.

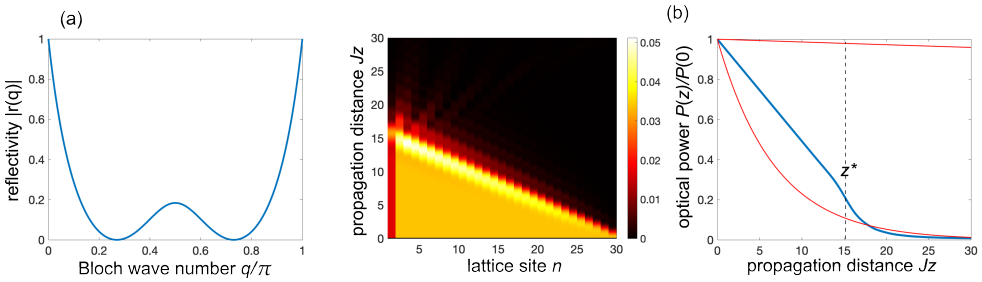


Figure 5. (**a**) Spectral reflection in a semi-infinite lattice with $N = 2$ boundary lossy sites ($\gamma_1 = \gamma_2 = \gamma$, $\gamma_n = 0$ for $n > 2$), for a loss rate $\gamma/J = 0.5$. The normalized Henrici parameter is $\nu_N = 0.0126$. Note that CPA occurs at the excitation Bloch wave numbers $q \simeq 0.27\pi$ and $q \simeq 0.72\pi$. (**b**) Light dynamics in a waveguide array comprising $L = 30$ waveguides with the two boundary lossy waveguides for an incident wave with Bloch wave number $q = 0.27\pi$, corresponding to the CPA condition. The right panel shows the light intensity propagation along the z axis on a pseudocolor map, whereas the right panels (blue bold curve) shows the numerically-computed decay dynamics of the total optical power $P(z)$. The thin red curves show the exponential decay curves corresponding to the most and less damped super-modes. The propagation distance z^*, above which the power decay deviates from the linear theoretical prediction, is $z^* = L/(2J)$.

5. Conclusions and Discussion

In summary, we have shown that non-normality in simple passive photonic lattices enables absorption dynamics that fundamentally deviate from the exponential laws dictated by orthogonal-mode systems. A uniform waveguide array containing loss at only one or a few sites near an edge can exhibit an algebraic, nearly linear decay of optical power when the input excitation is appropriately tailored. The algebraic decay is a clear signature of non-normal transport and originates from a CPA condition, which provides the specific excitation that ensures maximal, reflectionless energy flux toward the lossy boundary in the semi-infinite limit. Such a decay law is of interest because it enables a more uniform extraction of optical power along the propagation direction than conventional exponential attenuation, which is characterized by rapid initial power depletion followed by a long residual tail. The possibility of controlling how energy is dissipated, rather than merely the overall amount of absorption, provides an additional degree of freedom for the design of photonic transport and attenuation processes.

By analytically characterizing the dynamics for the minimal model of a single lossy edge site, and subsequently extending the analysis to multiple lossy sites, we have identified the precise conditions under which algebraic attenuation is sustained. In particular, we have demonstrated that the excitation condition yielding algebraic decay is realized when the system parameters approach a spectral singularity associated with coherent perfect absorption in the semi-infinite limit at the Bragg incidence angle. In this regime, the excitation matching the CPA condition is fully extinguished through constructive interference of non-orthogonal modes, giving rise to a distinctive algebraic decay law that persists over long propagation distances. More generally, our results highlight the broader role of non-normality as a resource for programmable energy flow in non-Hermitian photonic systems. Unlike traditional absorber engineering—where attenuation is dictated by spatial patterning—here the absorption law is governed primarily by modal interference and can be controlled through the input excitation. This suggests that even structurally simple dissipative lattices can be endowed with tunable, non-Lambertian attenuation behavior without requiring geometric modifications or additional functional layers.

Looking forward, the mechanism unveiled here suggests several extensions. The ability to tailor absorption through state preparation may offer practical advantages in integrated photonics, particularly in situations where non-exponential attenuation is desirable. Since the effect relies on modal non-orthogonality rather than on a specific physical im-

plementation, similar behavior may arise in other non-normal wave systems. Moreover, controlled proximity to spectral singularities could provide simple routes toward enhanced or selective absorption. Extensions involving gain–loss balance or dynamic modulation may further enrich the accessible absorption laws, although these directions lie beyond the scope of the present work.

Overall, the present work establishes algebraic absorption in passive non-Hermitian lattices as a robust and conceptually new phenomenon. Unlike conventional absorption mechanisms, which primarily control the magnitude of attenuation, the mechanism reported here enables control over the functional form of the absorption law itself through non-normal modal interference. Our results demonstrate that non-normality and spectral singularities provide powerful tools for shaping light–matter interactions and energy flow in minimally complex photonic structures, opening new perspectives for the engineering of unconventional attenuation dynamics in photonic and wave-based systems.

Funding: This research was partly funded by Agencia Estatal de Investigacion (MDM-2017-0711).

Data Availability Statement: No data were generated or analyzed in the presented research.

Conflicts of Interest: The author declares no conflicts of interest.

References

1. Feng, L.; El-Ganainy, R.; Ge, L. Non-Hermitian photonics based on parity-time symmetry. *Nat. Photonics* **2017**, *11*, 752. [CrossRef]
2. El-Ganainy, R.; Makris, K.G.; Khajavikhan, M.; Musslimani, Z.H.; Rotter, S.; Christodoulides, D.N. Non-Hermitian physics and PT symmetry. *Nat. Phys.* **2018**, *14*, 11. [CrossRef]
3. Longhi, S. Parity-time symmetry meets photonics: A new twist in non-Hermitian optics. *Europhys. Lett.* **2017**, *120*, 64001. [CrossRef]
4. Miri, M.-A.; Alu, A. Exceptional points in optics and photonics. *Science* **2019**, *363*, eaar7709. [CrossRef]
5. Ozdemir, S.K.; Rotter, S.; Nori, F.; Yang, L. Parity-time symmetry and non-Hermitian physics in optics and photonics. *Nat. Mater.* **2019**, *18*, 783. [CrossRef] [PubMed]
6. Midya, B.; Zhao, H.; Feng, L. Non-Hermitian photonics and topological phases in optical systems. *Nat. Commun.* **2018**, *9*, 2674. [CrossRef]
7. Wang, C.; Fu, Z.; Mao, W.; Qie, J.; Stone, A.D.; Yang, L. Non-Hermitian optics and photonics: From classical to quantum. *Adv. Opt. Photonics* **2023**, *15*, 442–523. [CrossRef]
8. Wang, Q.; Chong, Y.D. Non-Hermitian photonic lattices: Tutorial. *J. Opt. Soc. Am. B* **2023**, *40*, 1443–1466. [CrossRef]
9. Chen, S.; Basit, A.; Li, L.; Hou, C.; Ruan, Y.; Wei, Y.; Ni, Z. Non-Hermitian topological lattice photonics: An analytic perspective. *Adv. Photonics Res.* **2025**, *6*, 2500083. [CrossRef]
10. Xiao, L.; Wang, K.; Qu, D.; Gao, H.; Lin, Q.; Bian, Z.; Zhan, X.; Xue, P. Non-Hermitian physics in photonic systems. *Photonics Insights* **2025**, *4*, R09. [CrossRef]
11. Mostafazadeh, A. Spectral singularities of complex scattering potentials and infinite reflection and transmission coefficients at real energies. *Phys. Rev. Lett.* **2009**, *102*, 220402. [CrossRef] [PubMed]
12. Longhi, S. Spectral singularities in a non-Hermitian Friedrichs-Fano-Anderson model. *Phys. Rev. B* **2009**, *80*, 165125. [CrossRef]
13. Longhi, S. Spectral singularities and Bragg scattering in complex crystals. *Phys. Rev. A* **2010**, *81*, 022102. [CrossRef]
14. Mostafazadeh, A. Optical spectral singularities as threshold resonances. *Phys. Rev. A* **2011**, *83*, 045801. [CrossRef]
15. Jin, L. Asymmetric lasing at spectral singularities. *Phys. Rev. A* **2018**, *97*, 033840. [CrossRef]
16. Ghatak, A.; Nathan, J.A.; Mandal, B.P.; Ahmed, Z. Spectral singularity and reflectionlessness in non-Hermitian (complex) Ginocchio potential. *J. Phys. A Math. Theor.* **2012**, *45*, 465305. [CrossRef]
17. Long, D.; Zhu, J.; Mao, X.; Qin, G.-Q.; Wang, M.; Li, G.-Q.; Bo, F.; Long, G.-L. Exceptional-point-enhanced nanoparticle sensor utilizing a linewidth broadening mechanism. *Opt. Lett.* **2025**, *50*, 852–855. [CrossRef]
18. Long, D.; Mao, X.; Qin, G.-Q.; Wang, M.; Xie, R.-R.; Li, G.-Q.; Long, G.-L. Generation of unstable states via encircling exceptional nexus. *Opt. Express* **2025**, *33*, 9294–9305. [CrossRef]
19. Ahmed, Z. Reciprocity and unitarity in scattering from a non-Hermitian complex PT-symmetric potential. *Phys. Lett. A* **2013**, *377*, 957–960. [CrossRef]
20. Longhi, S. Invisibility in non-Hermitian tight-binding lattices. *Phys. Rev. A* **2010**, *82*, 032111. [CrossRef]
21. Longhi, S.; Gatti, D.; Della Valle, G. Non-Hermitian transparency and one-way transport in low-dimensional lattices by an imaginary gauge field. *Phys. Rev. B* **2015**, *92*, 094204. [CrossRef]

22. Zhang, X.Z.; Jin, L.; Song, Z. Perfect state transfer in $\mathcal{PT}$-symmetric non-Hermitian networks. *Phys. Rev. A* **2012**, *85*, 012106. [CrossRef]
23. Basiri, A.; Bromberg, Y.; Yamilov, A.; Cao, H.; Kottos, T. Light localization induced by a random imaginary refractive index. *Phys. Rev. A* **2014**, *90*, 043815. [CrossRef]
24. Longhi, S. Topological phase transition in non-Hermitian quasicrystals. *Phys. Rev. Lett.* **2019**, *122*, 237601. [CrossRef] [PubMed]
25. Tzortzakakis, A.F.; Makris, K.G.; Economou, E.N. Non-Hermitian disorder in two-dimensional optical lattices. *Phys. Rev. B* **2020**, *101*, 014202. [CrossRef]
26. Tzortzakakis, A.F.; Makris, K.G.; Szameit, A.; Economou, E.N. Transport and spectral features in non-Hermitian open systems. *Phys. Rev. Res.* **2021**, *3*, 013208. [CrossRef]
27. Weidemann, S.; Kremer, M.; Longhi, S.; Szameit, A. Coexistence of dynamical delocalization and spectral localization through stochastic dissipation. *Nat. Photonics* **2021**, *15*, 576. [CrossRef]
28. Longhi, S. Non-Hermitian control of localization in mosaic photonic lattices. *Appl. Phys. Lett.* **2023**, *123*, 161102. [CrossRef]
29. Li, B.; Chen, C.; Wang, Z. Universal non-Hermitian transport in disordered systems. *Phys. Rev. Lett.* **2025**, *135*, 033802. [CrossRef]
30. Longhi, S. Lifshitz tail states in non-Hermitian disordered photonic lattices. *Opt. Lett.* **2025**, *50*, 746. [CrossRef] [PubMed]
31. Yariv, A. Universal relations for coupling of optical power between microresonators and dielectric waveguides. *Electron. Lett.* **2000**, *36*, 321. [CrossRef]
32. Cai, M.; Painter, O.; Vahala, K.J. Observation of critical coupling in a fiber taper to a silica-microsphere whispering-gallery mode system. *Phys. Rev. Lett.* **2000**, *85*, 74. [CrossRef]
33. Kippenberg, T.J.; Spillane, S.M.; Vahala, K.J. Modal coupling in traveling-wave resonators. *Opt. Lett.* **2002**, *27*, 1669. [CrossRef]
34. Piper, J.R.; Liu, V.; Fan, S. Total absorption by degenerate critical coupling. *Appl. Phys. Lett.* **2014**, *104*, 251110. [CrossRef]
35. Piper, J.R.; Fan, S. Total absorption in a graphene monolayer in the optical regime by critical coupling with a photonic crystal guided resonance. *ACS Photonics* **2014**, *1*, 347. [CrossRef]
36. Chong, Y.D.; Ge, L.; Cao, H.; Stone, A.D. Coherent perfect absorbers: Time-reversed lasers. *Phys. Rev. Lett.* **2010**, *105*, 053901. [CrossRef]
37. Longhi, S. PT-symmetric laser-absorber. *Phys. Rev. A* **2010**, *82*, 031801. [CrossRef]
38. Wan, W.; Chong, Y.; Ge, L.; Noh, H.; Stone, A.D.; Cao, H. Time-reversed lasing and interferometric control of absorption. *Science* **2011**, *331*, 889. [CrossRef]
39. Longhi, S. Coherent perfect absorption in a homogeneously broadened two-level medium. *Phys. Rev. A* **2011**, *83*, 055804. [CrossRef]
40. Chong, Y.D.; Ge, L.; Stone, A.D. PT-symmetry breaking and laser-absorber modes in optical scattering systems. *Phys. Rev. Lett.* **2011**, *106*, 093902. [CrossRef] [PubMed]
41. Noh, H.; Chong, Y.; Stone, A.D.; Cao, H. Perfect coupling of light to surface plasmons by coherent absorption. *Phys. Rev. Lett.* **2012**, *108*, 186805. [CrossRef]
42. Longhi, S. Backward lasing yields a perfect absorber *Physics* **2010**, *3*, 61.
43. Sun, Y.; Tan, W.; Li, H.-Q.; Li, J.; Chen, H. Experimental demonstration of a coherent perfect absorber with PT phase transition. *Phys. Rev. Lett.* **2014**, *112*, 143903. [CrossRef] [PubMed]
44. Longhi, S.; Feng, L. PT-symmetric microring laser-absorber. *Opt. Lett.* **2014**, *39*, 5026. [CrossRef] [PubMed]
45. Wong, Z.J.; Xu, Y.L.; Kim, J.; O'Brien, K.; Wang, Y.; Feng, L.; Zhang, X. Lasing and anti-lasing in a single cavity. *Nat. Photonics* **2016**, *10*, 796. [CrossRef]
46. Li, H.; Suwunnarat, S.; Fleischmann, R.; Schanz, H.; Kottos, T. Random Matrix Theory Approach to Chaotic Coherent Perfect Absorbers. *Phys. Rev. Lett.* **2017**, *118*, 044101. [CrossRef]
47. Suwunnarat, S.; Halpern, D.; Li, H.; Shapiro, B.; Kottos, T. Dynamically modulated perfect absorbers. *Phys. Rev. A* **2019**, *99*, 013834. [CrossRef]
48. Wang, C.; Sweeney, W.R.; Stone, A.D.; Yang, L. Coherent perfect absorption at an exceptional point. *Science* **2021**, *373*, 1261. [CrossRef]
49. Horner, H.; Wild, L.; Slobodkin, Y.; Weinberg, G.; Katz, O.; Rotter, S. Coherent perfect absorption of arbitrary wavefronts at an exceptional point. *Phys. Rev. Lett.* **2024**, *133*, 173801. [CrossRef]
50. Xu, H.S.; Jin, L. Robust incoherent perfect absorption. *Phys. Rev. Res.* **2024**, *6*, L022006. [CrossRef]
51. Xu, H.; Wang, L.; Yuan, L.; Jin, L. High-order perfect absorption in the absence of exceptional point. *Phys. Rev. Lett.* **2026**, *136*, 136902. [CrossRef]
52. Higgins, K.D.B.; Benjamin, S.C.; Stace, T.M.; Milburn, G.J.; Lovett, B.W.; Gauger, E.M. Superabsorption of light via quantum engineering. *Nat. Commun.* **2014**, *5*, 4705. [CrossRef]
53. Yang, D.; Oh, S.H.; Han, J.; Son, G.; Kim, J.; Kim, J.; Lee, M.; An, K. Realization of superabsorption by time reversal of superradiance. *Nat. Photonics* **2021**, *15*, 272–276. [CrossRef]
54. Li, H.; Alú, A. Temporal switching to extend the bandwidth of thin absorbers. *Optica* **2021**, *8*, 24–29. [CrossRef]

55. Siegman, A.E. Excess spontaneous emission in non-Hermitian optical systems. I. Laser amplifiers. *Phys. Rev. A* **1989**, *39*, 1253. [CrossRef]
56. Cheng, Y.-J.; Fanning, C.G.; Siegman, A.E. Experimental observation of a large excess quantum noise factor in the linewidth of a laser oscillator having nonorthogonal modes. *Phys. Rev. Lett.* **1996**, *77*, 627. [CrossRef]
57. Siegman, A.E. Propagating modes in gain-guided optical fibers. *J. Opt. Soc. Am. A* **2003**, *20*, 1617. [CrossRef]
58. Berry, M.V. Mode degeneracies and the Petermann excess-noise factor for unstable lasers. *J. Mod. Opt.* **2003**, *50*, 63. [CrossRef]
59. Longhi, S.; Laporta, P. Excess noise in intracavity laser frequency modulation. *Phys. Rev. E* **2000**, *61*, R989. [CrossRef]
60. Longhi, S. Enhanced excess noise in laser cavities with tilted mirrors. *Opt. Lett.* **2000**, *25*, 811–813. [CrossRef]
61. Firth, W.J.; Yao, A.M. Giant excess noise and transient gain in misaligned laser cavities. *Phys. Rev. Lett.* **2005**, *95*, 073903. [CrossRef]
62. Papoff, F.; D'Alessandro, G.; Oppo, G.L. State-dependent pseudoresonances and excess noise. *Phys. Rev. Lett.* **2008**, *100*, 123905. [CrossRef] [PubMed]
63. Makris, K.G.; Ge, L.; Türeci, H.E. Anomalous transient amplification of waves in non-normal photonic media. *Phys. Rev. X* **2014**, *4*, 041044. [CrossRef]
64. Longhi, S. PT-symmetric quantum oscillator in an optical cavity. *EPL* **2016**, *115*, 61001. [CrossRef]
65. Longhi, S. Anomalous dynamics in multilevel quantum decay. *Phys. Rev. A* **2018**, *98*, 022134. [CrossRef]
66. Longhi, S. Quantum Mpemba effect from non-normal dynamics. *Entropy* **2025**, *27*, 581. [CrossRef] [PubMed]
67. Asllani, M.; Lambiotte, R.; Carletti, T. Structure and dynamical behavior of non-normal networks. *Sci. Adv.* **2018**, *4*, eaau9403. [CrossRef]
68. Henrici, P. Bounds for Iterates, Inverses, Spectral Variation and Fields of Values of Non-Normal Matrices. *Numer. Math.* **1962**, *4*, 24. [CrossRef]
69. Lambropoulos, K.; Simserides, C. Spectral and transmission properties of periodic 1D tight-binding lattices with a generic unit cell: An analysis within the transfer matrix approach. *J. Phys. Commun.* **2018**, *2*, 035013. [CrossRef]

Disclaimer/Publisher's Note: The statements, opinions and data contained in all publications are solely those of the individual author(s) and contributor(s) and not of MDPI and/or the editor(s). MDPI and/or the editor(s) disclaim responsibility for any injury to people or property resulting from any ideas, methods, instructions or products referred to in the content.